Volume 1 | Number 1 | Jan 2013 | Pages 1–100

Journal of
Materials Chemistry C

Materials for optical and electronic devices
www.rsc.org/materialsC

ROYAL SOCIETY
OF CHEMISTRY

ROYAL SOCIETY
OF CHEMISTRY

www.rsc.org/materialsC

Journal Name

ARTICLE

Surface plasmonic spectroscopy revealing the oxidation dynamics of copper nanowires embedded in polycarbonate ion-track templates

Jinglai Duan[a,b], Jie Liu[a], Yongliang Zhang[b], Christina Trautmann[c,d], Dang Yuan Lei[*b,e]

Chemical stability of metal nanowires is a great concern for many practical applications. Metal nanowires deposited in the pores of various templates have been considered oxidization-resistant because the templates provide natural protection. Here we present the first ever attempt to investigate the oxidation behavior of copper nanowires supported in a template matrix using a surface-plasmon-based optical spectroscopy method combined with high-resolution transmission electron microscope (TEM). Although the nanowires are protected by being embedded in the polymer template matrix, unexpected oxidation is clearly observed in TEM imaging, which unambiguously reveals the possible underlying oxidation mechanism responsible for the oxidation passivation. By measuring the optical properties with localized surface plasmon resonance spectroscopy, the oxidation behavior of the copper nanowires is studied as a function of storage time in both air and vacuum and thus uncovers the oxidation dynamics of copper. Finally, we demonstrate that the oxidation can be entirely prevented by sealing the open ends of the wires, which is confirmed by monitoring the electrical resistance of single nanowires. Our results have significant importance in understanding the oxidation behavior of metal nanostructures in general and also provide useful guidelines to estimate the electrical functionality of them used in optoelectronic devices.

Introduction

Metallic nanowires have attracted enormous attention since they open up exciting applications in the fields of electronics, plasmonics, sensors, green energy, and many more.[1-6] For instance, metal nanowires made of copper[7-9] and silver[10,11] are promising transparent electrodes in optoelectronic devices such as thin film solar cells, flat panel displays, organic light-emitting diodes (OLEDs), and touch-screens. Furthermore, as electronic device features are pushed towards the deep sub-100-nm regime, metallic nanowires are considered as ideal candidates for functional building blocks and interconnections.[12-14] In order to maintain their excellent functionalities, metallic nanowires should be either chemically inert or chemically protected. Due to the large surface-area-to-volume ratio, however, they show enhanced chemical activity compared to their bulk counterparts and therefore are more easily susceptible to oxidization.[15] Hence, the sheet resistance of copper nanowire transparent electrode was gradually increased as time elapses because of natural oxidation of

copper. Within 28 days, the sheet resistance increased from initially ~1 Ohm/sq up to ~16 Ohm/sq, corresponding to a gain factor of 16.[7] In many applications, such a high increase in electrical resistance is unfavorable for long-term applications in optoelectronic devices. To sustain persistent functional performance of devices, oxidation has to be eliminated by protection during use, storage, and transportation.

It is well known that the oxidation of metal nanowires is highly dependent on fabrication method. In the past decades, various strategies, including template-free and template-based methods, have been developed to successfully prepare metallic nanowires with designed properties. Especially, template-based methods using anodic oxide aluminum (AAO) and porous nuclear track membrane (PNTM) templates have been extensively applied. The importance and popularity of template-based methods are well reflected by the large number of relevant publications. Using "template" and "nanowire" as search keywords, 89,100 results are returned by Google Scholar[@] and 8,929 by ISI Web of Science[@], respectively (data obtained as accessed on November 10th, 2015). These voluminous research databases provide ample testimony of enormous scientific interest in and technological importance of template-based nanowires. In contrary to the fast increasing investigations on synthesis, characterizations, and applications of metallic nanowires, less attention has been paid to their oxidation issue. This issue has been largely overlooked in the past probably because the metal nanowires have been considered to be natively protected by the template matrices, both mechanically and chemically. However, there is

[a] Materials Research Center, Institute of Modern Physics, Chinese Academy of Sciences, Lanzhou 730000, P. R. China.
[b] Department of Applied Physics, The Hong Kong Polytechnic University, Hong Kong, China. *Email: dylei@polyu.edu.hk (DYL)
[c] Materials Research Department, GSI Helmholtz Centre for Heavy Ion Research, 64291 Darmstadt, Germany
[d] Materials Science, Technische Universität Darmstadt, 64287 Darmstadt, Germany
[e] Shenzhen Research Institute, The Hong Kong Polytechnic University, Shenzhen, China

the important question if a template matrix really provides a safe harbor for metallic wires to prevent oxidation. The answer to this question and the solution to this general issue are the theme of the present invited contribution. In fact, the oxidation issue is also common for metal nanowires prepared with template-free methods, such as chemical vapor deposition (CVD)[15] and solution chemical reaction,[7] because the as-prepared nanowires usually have high surface activities and therefore can be very susceptible to oxidation. In order to alleviate suffering from post-oxidation, additional surface decorations with inert materials were commonly introduced in the template-free methods.[15]

In this work, we present the first study to demonstrate that metal nanowires can still get oxidized despite being embedded in template matrices. Using a surface-plasmon-based optical spectroscopy together with high-resolution TEM (HRTEM) imaging, we uncover the oxidization dynamics of copper nanowires and propose a possible mechanism. The optical measurement results of the oxidation dynamics are further corroborated by full-wave numerical simulations. We finally show that the oxidation process can be alleviated by storing the nanowires in low pressure vacuum and further completely prevented by sealing the surface of the template matrices, demonstrating a constant electrical resistance over a long storage period.

Experimental section

Copper nanowires were electrochemically synthesized in home-made polycarbonate (PC) ion-track templates, with the detailed preparation procedure described elsewhere.[16] The irradiation of the PC foils was carried out at the Heavy Ion Research Facility in Lanzhou (Lanzhou, China) with 9.5 MeV/u [209]Bi ions and at the UNILAC linear accelerator of GSI (Darmstadt, Germany) with 11.1 MeV/u Pb ions. The irradiation fluence was 1×10^8 ions·cm^{-2} for preparation of nanowire arrays and one ion hit for preparation of single nanowires, respectively. In the electrochemical deposition of copper, a thin layer of sputtered gold reinforced with a ~10 um thick copper layer served both as cathode and supporting substrate (gold/copper substrate). The electrolyte consisted of an aqueous solution of 75 g/l $CuSO_4 \cdot 5H_2O$ and 30 g/l H_2SO_4. A copper rod of 2 mm in diameter was used as anode. The applied voltage for electrochemical deposition of copper was 200 mV and the deposition temperature was kept at 50 ºC. The length of the nanowires was controlled by the deposition time. To release the deposited nanowires from the template, the PC matrix was dissolved in dichloromethane (CH_2Cl_2). The Cu nanowire arrays were examined with scanning electron microscopy (SEM, Philips XL30), transmission electron microscopy (TEM, JEOL JEM-3010 and FEI Tecnai G2 F30), and selected area electron diffraction (SAED). In the optical extinction measurement, the substrate and wire caps (grown on the upper template surface once the pores were completely filled) were mechanically detached with forceps[17] and an UV-Vis-NIR spectroscopy (Perkin-Elmer, Lambda 900) was employed to record the optical spectra of the sample. The

electrical resistance of single nanowires was measured using a broad purpose source meter (Keithley, Model 2400). In order to monitor the resistance a thin gold film with thickness of ~100 nm was coated on the top surface of the template by sputtering. This sputtered gold film provided an electrical contact to the cap of the single nanowire and served as electrode, whereas the gold/copper substrate was the counter electrode.

Results and discussion

The morphological properties of Cu nanowires were examined over large areas by SEM. The SEM micrographs shown in Figures 1a and 1b demonstrate that both short (~2 um) and long nanowires have an excellent cylinder shape with uniform diameter over the full wire length. The diameter of the prepared nanowires is about 75 nm, corresponding to the applied track etching protocol. Figure 1a shows that the short nanowires are vertically aligned on the substrate, revealing that the nanowires produced by ion-track template method are originally parallel to each other when they are embedded in template and all the wires are perpendicular to template surface. Such an identical special arrangement is critical to the following optical measurements. The wires obtained by completely filling the nanopores had a length of 30 μm. Due to the large length-to-diameter ratio, these nanowires collapse on the substrate as shown in Figure 1b.
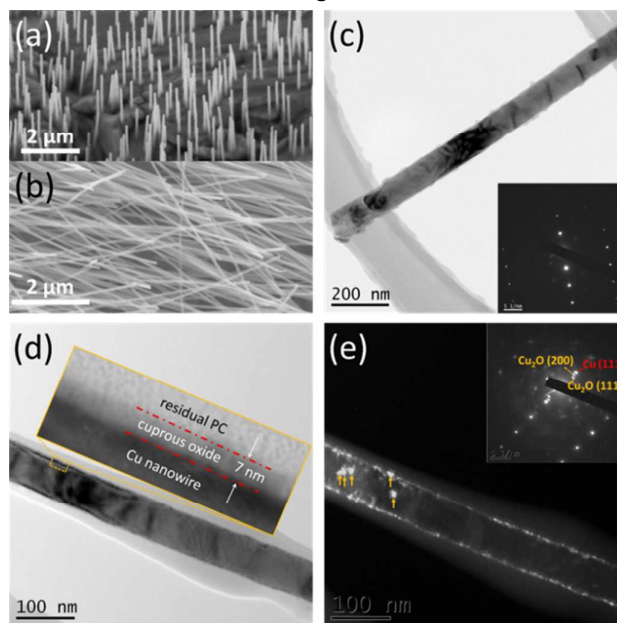
Figure 1. SEM and TEM analysis of Cu nanowires. (a) SEM micrograph of an array of short copper nanowires, which are vertically aligned on an Au/Cu substrate and have a length of 2 μm. (b) SEM image of an array of 30 μm long copper nanowires, which collapse on the substrate due to large length-to-diameter ratio. (c) Representative TEM image and the corresponding SAED pattern (inset) of a freshly prepared copper nanowire, exhibiting single-crystalline structure and no oxide formed. (d) Representative TEM image of nanowire after

10 months of storage in air, showing a ~7 nm thick cuprous oxide surface layer. (e) TEM dark-field image and SAED pattern corresponding to same nanowire shown in (d), the light islands on surface consist of Cu_2O as confirmed by SAED pattern.

The microstructural characterizations of a freshly prepared copper nanowire stored in vacuum or air were carried out by TEM and electron diffraction. The nanowires were left embedded in their host templates until TEM experiments. To avoid possible oxidization during sample preparation for TEM measurements, the nanowires were immediately transferred into the TEM sample chamber after taking them out from dichloromethane solution. Figure 1c shows a representative TEM micrograph and the corresponding SAED pattern of a freshly prepared nanowire. The TEM bright-field image demonstrates that the fresh nanowire has a smooth cylinder shape as observed in the SEM image and that no oxide layer is formed on the surface. The SAED pattern shown in the inset further confirms that the nanowire has a pure single-crystalline phase that is indexed as a face centered cubic (fcc) plane. These results clearly evidence that the fresh nanowire has not been oxidized.

For a copper nanowire after exposure in air for 10 months, the TEM bright-field image in Figure 1d shows that a new layer assigned as cuprous oxide is formed on the copper surface. The outermost layer is ascribed to the residual polycarbonate on the nanowire as frequently observed.[17] The enlarged area shown in Figure 1d uncovers clearly the thin oxide layer with ~7-nm thickness between the residual PC and the copper surface. The TEM dark-field image shown in Figure 1e further discloses that the oxide layer is formed only on the surface of the copper nanowire, distributed along the whole wire length, and composed of small grains (light islands). The two sets of electron diffraction signals in the SAED pattern (inset of Figure 1e) strongly evidence the coexistence of single-crystalline Cu, corresponding to the bright set of diffraction pattern, and polycrystalline Cu_2O to the weak set. In addition, there are also some obvious Cu_2O islands formed on the surface, as indicated by the yellow arrows in the TEM image.

It is worthwhile mentioning that only Cu_2O rather than CuO was observed in the sample. The topographical and structural characteristics of Cu_2O are further investigated by HRTEM. As shown in the lattice mapping in Figure 2, two material phases are clearly observed and separated by an interfacial layer. The densely-packed lattice fringes on the left side of the HRTEM image have a lattice spacing of 0.209 nm and are identified as the (111) crystal planes of Cu (ref. Cu PDF card no. 04-0836), further confirming the single crystalline structure of copper as revealed by the electron diffraction pattern shown in Figure 1. Also on the right side of the lattice mapping, the lattice spacing varies from 0.236 to 0.246 nm at different areas and the crystal plane can be indexed to the (111) plane of Cu_2O (ref. Cu_2O PDF card no. 78-2076). It is important to note that the most part of the Cu_2O (111) plane are parallel to the Cu (111) plane, demonstrating an epitaxial growth of Cu_2O. However, due to the significant lattice mismatch between Cu and Cu_2O, some edge dislocations, as indicated by the "⊤" symbols in Figure 2, are observed in the vicinity of the Cu/Cu_2O interface.

In addition, a small region of lattice distortion enclosed within the dash-dotted ellipse is also observed in the epitaxial Cu_2O region. The appearance of the distorted lattices can be attributed to the local hetero-epitaxial strain field induced by the lattice misfit of Cu and Cu_2O. It is also noteworthy to mention that, besides the epitaxial Cu_2O, two adjacent Cu_2O grains as highlighted by the dotted ellipses were coalesced at the outer surface where a grain boundary was formed between the grains. The crystallographic orientations of the two grains are nearly parallel but different from that of the epitaxial Cu_2O.
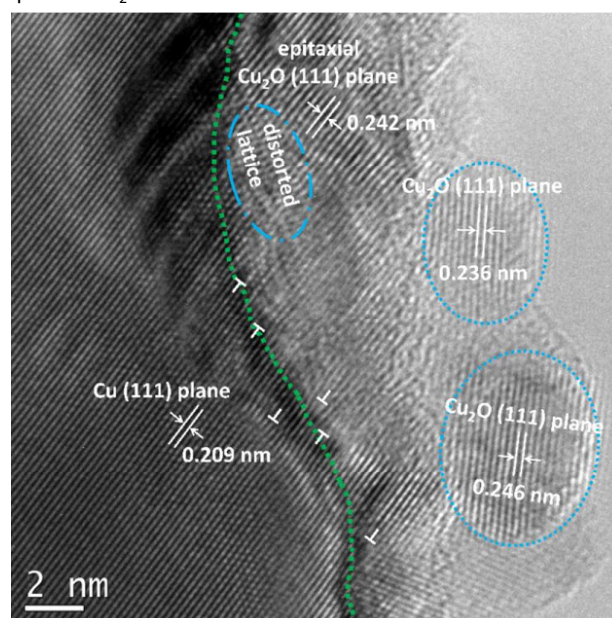
Figure 2. High resolution TEM image of a Cu nanowire stored for 10 months in air. The densely packed lattice fringes on the left side are indexed to single crystalline Cu whereas the ones on the right side are Cu_2O that comprises of an epitaxial layer and multiple polycrystalline Cu_2O grains with different crystallographic orientations (light-blue dotted circles). The oxidization converts the pure single crystalline Cu nanowire into a Cu/Cu_2O core/shell structure. The Cu/Cu_2O interface is indicated by the green dashed line. Due to the mismatch of lattice spacing between Cu and Cu_2O, some edge dislocations, denoted by "⊤" symbols, are observed in the vicinity of the interface. In addition, region of distorted lattices (DL) are formed (see dash-dotted ellipse).

Fundamental understanding of natural oxidation in metals has received extensive interest owning to its great technical importance.[18,19] In the classical theories, the growth of a thin film assumes two continuous stages, namely the formation and thickening of a continuous layer.[18] Whereas the modern theories propose that the metal oxidation process generally has three stages, involving oxygen surface chemisorption, nucleation and growth of oxide, and bulk oxide growth.[19-21] Previous theoretical and experimental studies on the oxidation of copper thin films suggest that oxygen surface diffusion, rather than bulk diffusion of Cu atoms, or oxygen diffusion into Cu followed by oxide nucleation within bulk Cu is the primary

mechanism of transport, nucleation, and growth of an oxide layer.[19,22] The formation of Cu_2O is complex and highly dependent on the conditions such as temperature and oxygen pressure. For example, because of the lower mobility of oxygen at low temperature, the nucleation of a new oxide nucleus is more favorable than the attachment to an existing island.[22] High oxygen pressure also facilitates the nucleation of emerging nuclei enabled by high oxygen adsorption flux.[23] In our experiment, the single-crystalline Cu nanowires embedded in the PC template matrices were stored in air at atmospheric pressure and room temperature. Compared to the elevated temperature of hundreds degrees centigrade and the high vacuum pressure (0.5-150 Torr) in the previous study by Luo et al.,[23] the present conditions are more beneficial for the formation of individual Cu_2O islands as observed in Figures 1e and 2. In addition to the increased nucleation rate, it was experimentally evidenced that a low oxygen pressure (0.5 Torr) favored only epitaxial nucleation of Cu_2O whereas high oxygen pressure (150 Torr) gives rise to the formation of both epitaxial and non-epitaxial Cu_2O. In the present work, the oxygen pressure was at the atmospheric level that ultimately induced the growth of both epitaxial and non-epitaxial Cu_2O grains as shown in Figure 2. Note that the structural features of pristine Cu, e.g. crystallographic orientation, crystallinity, surface roughness, and lattice defects, are additional factors influencing the formation of Cu_2O.[19]

The TEM characterization results shown above provide comprehensive understanding of the microscopic mechanism responsible for the oxidation behaviour of copper after storage for certain periods at specific conditions. Yet, it could be very tedious and time consuming to investigate the oxidation dynamics of the sample as a function of storage duration. To monitor the time-dependent oxidation behaviour in an efficient manner, here we apply the plasmon resonance based optical spectroscopy method that has been successfully used for monitoring nanoscale phase transition of VO_2.[24-26] This method utilizes the localized surface plasmon resonance (LSPR) sustained by subwavelength metallic objects. LSPR arises from collective oscillation of conduction electrons in noble metals and is highly sensitive to the change in surrounding environment, making it an ultrasensitive optical tool for sensing purposes.[27,28] In this work, we applied this spectroscopic technique to get insight into the oxidation kinetics as a function of storage time by measuring the LSPR spectra of Cu nanowire arrays embedded in template matrices. The LSPR spectra of wires stored in air were recorded day by day over a period of 10 days (Figure 3a). The configuration of the transmission measurement is schematically illustrated in the inset of Figure 3a.[28] The peak located at ~ 650 nm is assigned to a dipolar resonance at which the conduction electrons oscillate in the direction of the wire diameter, known as transverse mode.[28] As storage time elapses, the peak obviously shifts to red. The redshifts for 1 day and 10 days of storage are 6 nm and 10 nm, respectively. The red-shift of the peak as a function of oxidation time is plotted in Figure 3c. Given by the results from the TEM analysis, it is obvious that the oxidation of the nanowires occurs during storage. This

raises the question where the oxygen atoms come from. One possibility is that oxygen is produced during the electrochemical deposition process, e.g. via electrolysis of water and/or residual oxygen in the electrolytic solution. The
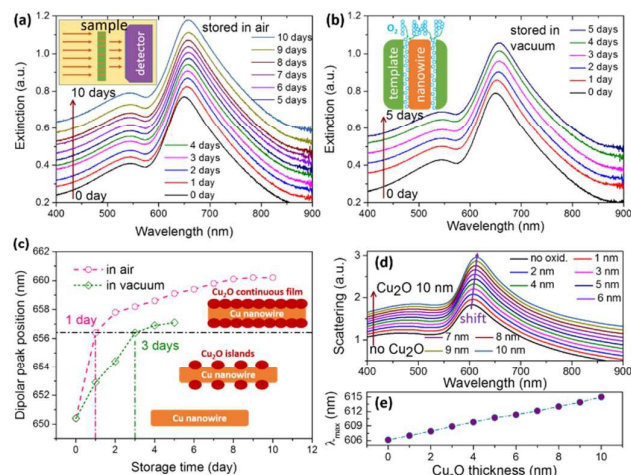
Figure 3. Plasmon resonance optical spectroscopy of oxidation dynamics of copper nanowires: experiment and simulation. (a) Ambient-environment-storage-time dependent extinction spectra of Cu nanowires embedded in template matrices. The sample was stored in air for 10 days. The inset shows the optical measurement setup. The continuous redshift of the dipolar LSPR peak reflects gradual oxidation of Cu. (b) Vacuum-storage-time dependent extinction spectra of embedded Cu nanowires. The sample was stored in a low-pressure vacuum (~ 200 Pa) for 5 days. The redshift of the dipolar LSPR peak is significantly slower than that for the sample stored in air. The inset schematically shows the diffusion of oxygen into the interface between the nanowire and the template. (c) Time dependent LSPR position of Cu nanowires extracted from the spectra in (a) and (b). For both storage environments, a peak shift of 6 nm (from ~650.5 nm to 656.5 nm) denotes the transition point at which discontinuous Cu_2O islands are coalesced to form continuous Cu_2O film that limits further oxidation by depressing oxygen diffusion. The inset schematically shows the morphological evolution of Cu_2O. (d & e) Electromagnetic simulation of scattering spectra of a Cu nanowire with diameter 85 nm (d) and extracted Cu_2O thickness-dependent LSPR position showing a linear relationship (e), illustrating the potential of using LSPR spectroscopy as an optical nanoruler to measure the thickness of Cu_2O.

oxygen may accumulate in gaps between the nanowire and the pore wall. Another possibility is oxygen from air via diffusion and penetration along the gaps between wire surface and pore wall. To clarify this issue, we measured the LSPR spectra of identical template-embedded Cu nanowire arrays in a low-pressure vacuum vessel with a pressure about 200 Pa. After preparation and after each optical measurement, the sample was immediately returned into vacuum. Figure 3b shows the storage time-dependent LSPR spectra of wires

stored in vacuum until 5 days and only exposed to air during the LSPR measurement and each exposure was about 20 minutes. It is obvious that the dipolar peak also shifts to red with increasing storage time (Figure 3c). The peak shift rate of the sample stored in vacuum is significantly slower than that of the sample stored in air. A peak shift of 6 nm occurs within 3 days for the sample stored in vacuum in contrast to one day for the sample stored in air. More importantly, after a shift of 6 nm is reached, the rate of the shifts significantly slows down independent of the storage environment. It is well known the LSPR of plasmonic structures is highly sensitive to the surrounding medium and an increase of the static dielectric constant (or refractive index) of the surrounding medium shifts the LSPR to red.[27,29,30] In this work, the initial surrounding medium of Cu nanowires is the polycarbonate template that has a static dielectric constant of 3. During oxidation of the nanowire surface the surrounding medium changes from PC to Cu_2O which has a larger static dielectric constant of 7.6. The increase in dielectric constant of the surrounding medium is assumed to be at least partially responsible for the redshift of the dipolar LSPR peak.[29] In addition, it has been reported that also a thickness increase of the surrounding medium leads to a LSPR redshift,[29,30] with the redshift increasing approximately linearly with medium thickness in the case that the thickness of medium is not too large (e.g. below 15 nm).[29] To clarify this point, we performed electromagnetic simulations and calculated the scattering cross sections with respect to the thickness of Cu_2O with a commercial electromagnetic solver FDTD Solutions. Since we are interested in the dipolar LSPRs across by the transverse section of the nanowires, we simplified the complex three-dimensional structure to a two-dimensional (2D) model, where a 2D core-shell of Cu and Cu_2O structure scatters the electromagnetic waves. In fact, the calculated cross sections correspond to the LSPR mode of nanowires with infinite length. By doing so, the huge computation effort required for our 3D core-shell geometries with extremely high aspect ratios (length 30 um over mesh size of 1 nm) can be significantly decreased. It should be noted that the calculated LSPRs are blue shifted compared to the modes of a 3D nanowire because of the neglect of the phase delaying effect. The total-field / scattered-field formulation is used to extract the scattered field from the incident wave. Four perfectly matched layers in the surrounding space have been employed to minimize the reflection. In the simulations, the diameter of the nanowire is set equal to 85 nm, while the thickness of Cu_2O increases from 0 to 10 nm. The simulated spectra shown in Figure 3d reveal that, with increasing the thickness of Cu_2O, the dipolar LSPR peak shifts clearly to the red (figure 3d). The peak shift as a function of Cu_2O thickness (figure 3e) shows a linear relationship, at least up to a layer of 10 nm. This allows us to use the position of the LSPR signal as an optical ruler for measuring the oxide thickness of Cu nanowires. Taking advantages of this correlation, we analyzed the oxidation kinetics of Cu nanowires embedded in PC template matrices stored in air and in vacuum. For the samples stored in air, the largest peak shift occurs within the first day. In contrast, samples stored in vacuum show the same peak shi
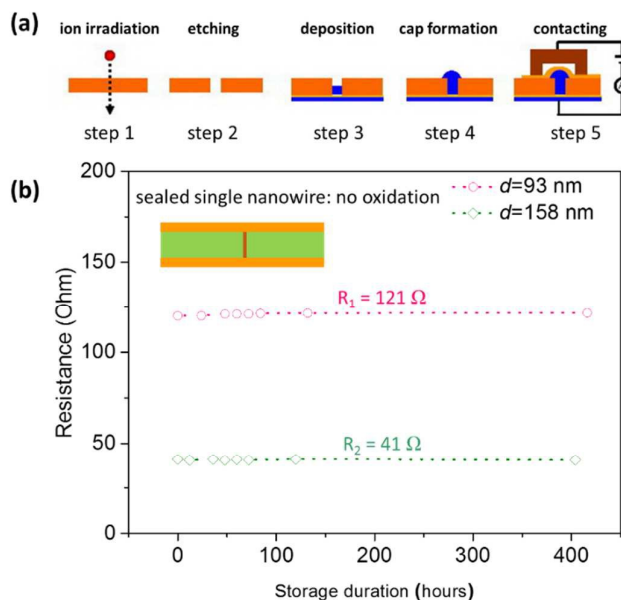
Figure 4. (a) Schematics of fabrication procedure of single nanowires consisting of membrane irradiation with a single ion (step 1), converting the ion track into an open nanopore by chemical etching (step 2), electrochemical deposition of copper into nanopore (step 3), intentional cap formation by overgrowth (step 4), and electrical contact of single nanowires (step 5). (b) Electrical resistance of two templates containing a single Cu nanowire sealed by thin gold films (inset) as a function of storage time. Monitoring the resistance over 400 h shows no significant change indicating that oxidation is successfully prevented by sealing the wires in the template (inset).

shift within the first three days. In vacuum, the oxidation is obviously depressed indicating that the oxygen mainly comes from air by diffusion and penetration, as schematically demonstrated in the inset of Figure 3b. In Figure 3c, both peak shifts slow down after a critical oxide layer of 6 nm, evidencing that subsequent oxidation is strongly reduced. It has been reported that the formation of Cu_2O layers of Cu films has two stages, i.e. formation of Cu_2O islands and coalescence of islands to form continuous oxide layers.[19] Once a continuous oxide layer is formed, further oxidation is self-limited because the continuous oxide layer hinders oxygen diffusion and thus further growth of existing islands and the formation of new islands.[31] Our results suggest that the oxidation of Cu nanowires also follows the kinetics of Cu film oxidation.

For practical applications of metal nanowires, oxidation should be completely prevented. During storage, the oxygen source is ambient air; we therefore propose a simple route to solve the problem by sealing both open ends of the wires. We thus encapsulated the wires between sputtered gold films (~ 100 nm in thickness) on both surfaces of the templates as schematically shown by the inset of Figure 4. Optical examination is no longer valid because visible light cannot penetrate into sample excluding LSPR excitation. As an

alternative method thus electrical measurements were performed expecting higher wire resistance if oxidation occurs. In the case of single nanowires, this method is sensitive because the oxidation induced resistance change is sufficiently high to be detected. For instance, the resistance of a single nanowire of 30 μm in length and 93 nm in diameter is 121 Ohm (see Figure 4b). For a 1-nm in thick oxidation layer the resistance increase will be 5.8 Ohm which can easily be detected. To fabricate and electrically contact single Cu nanowires five main steps are involved (Figure 4a).[32] First, a 30-μm thick PC foil was irradiated with one single high-energy heavy ion (e.g. 1 GeV Au ion) (step 1). By chemical etching the ion track was converted into a single nanopore (step 2). Then the pore was filled by electrochemical deposition using a gold/copper electrode on the substrate as described for the wire array fabrication (step 3). Over growth (continue deposition when wire reaches the upper template surface) was intentionally employed in order to produce a large cap suitable as electrical contact (step 4). Finally, a thin gold film was sputtered onto the top surface allowing electrical measurements (step 5). Figure 4b shows the time evolution of the electrical resistances of two samples containing a single nanowire. The nanowire diameter is 93 and 158 nm and the respective resistance is 121 and 41 Ohm. For both wires, the resistances show no observable change over 400 hours, revealing that no oxidation occurred. These electrical measurements demonstrate that sealing with thin gold films provides a reliable protection for the wires despite the fact that the samples were stored in air. This finding also suggests that the oxidation problem can be completely prevented, and stable, sustainable functional performances can be expected for, for example, nanowire-based sensors, electronic devices, and transparent electrodes. We should mention here that, instead of using expensive gold, coating films of other cheaper metals (e.g. Cu), semiconductors, and polymers can also be used to prevent oxygen diffusion and penetration from atmospheric environment.

Conclusions

In conclusion, we demonstrated that oxidation of single-crystal Cu nanowire arrays occurs even if they are embedded in a polycarbonate template. The oxide formed on the nanowire surface is Cu_2O, and no evidence for CuO is found. High-resolution TEM imaging shows that Cu_2O is epitaxially grown on the Cu nanowire surface. Some crystal defects such as edge dislocations and lattice distortion form in the vicinity of the Cu/Cu_2O interface. Also some small Cu_2O grains with different crystallographic orientations are found. The LSPR spectra show a redshift of the dipolar LSPR peak that becomes larger with increasing the thickness of the Cu_2O layer. Electromagnetic simulations reveal a linear relationship of the peak shift and Cu_2O thickness. These results suggest that the shift of the LSPR peak may serve as an optical nanoruler for measuring the oxide thickness of nanowires. We also show that the oxygen source that induces oxidation originates mainly from air. Based on this finding, we propose two technical methods that effectively minimize the risk of oxidation: (i) oxidation can be limited by storing the samples in low pressure vacuum and (ii) oxidation can be prevented by sealing the open ends of the wires. Both methods are of technical importance for obtaining stable and sustainable functional performances of Cu nanowire-based sensors, electronic devices, and transparent electrodes.

References

1   Y. Peng and K. Kempa, *Appl. Phys. Lett.*, 2012, **100,** 171903.
2   X. Chen and R. H. Victora, *Appl. Phys. Lett.*, 2008, **93**, 162105.
3   H. Yoon, T. Kang, J. M. Lee, S. Kim, K. Seo, J. Kim, W. I. Park and B. Kim, *J. Phys. Chem. Lett.*, 2011, **2**, 956.
4   J. L. Duan, T. W. Cornelius, J. Liu, S. Karim, H. J. Yao, O. Picht, M. Rauber, S. Müller and R. Neumann, *J. Phys. Chem. C*, 2009, **113**, 13583.
5   J. Juarez, A. Cambon, S. Goy-Lopez, A. Topete, P. Taboada and V. Mosquera, *J. Phys. Chem. Lett.*, 2010, **1**, 2680.
6   Z. Y. Bao, D. Y Lei, R. Jiang, X. Liu, J. Dai, J. Wang, H. L. W. Chan and Y. H. Tsang, *Nanoscale*, 2014, **6**,9063.
7   A. R. Rathmell, S. M. Bergin, Y.-L. Hua, Z.-Y. Li and B. J. Wiley, *Adv. Mater*, 2010, **22**, 3558.
8   A. R. Rathmell and B. J. Wiley, *Adv. Mater*, 2011, **23**, 4798.
9   D. Zhang, R. Wang, M. Wen, D. Weng, X. Cui, J. Sun, H. Li and Y. Lu, *J. Am. Chem. Soc.*, 2012, **134**, 14283.
10 J.-Y. Lee, S. T. Connor, Y. Cui and P. Peumans, *Nano Lett.*, 2008, **8**, 689.
11 S. De, T. M. Higgins, P. E. Lyons, E. M. Doherty, P. N. Nirmalraj, W. J. Blau, J. J. Boland and J. N. Coleman, *ACS Nano*, 2009, **3**, 1767.
12 C. C. Yang, C. Witt, P. C. Wang, D. Edelstein and R. Rosenberg, *Appl. Phys. Lett.*, 2011, **98**, 051911.
13 K. Critchley, B. P. Khanal, M. L. Gorzny, L. Vigderman, S. D. Evans, E. R. Zubarev and N. A. Kotov, *Adv. Mater.*, 2010, **22**, 2338.
14 J. Li, Z. Zhou, X. Yang, W. Zhang, S. Sang and P. Li, *Small*, 2013, **9**, 3014.
15 D. Wang, Y. L. Chang, Z. Liu and H. Dai, *J. Am. Chem. Soc.*,2005, **127**, 11871.
16 J. Liu, J. L. Duan, M. E. Toimil-Molares, S. Karim, T. W. Cornelius, D. Dobrev, H. J. Yao, Y. M. Sun, M. D. Hou, D. Mo, Z. G. Wang and R. Neumann, *Nanotechnology*, 2006, **17**, 1922.
17 J. L. Duan, J. Liu, D. Mo, H. J. Yao, K. Maaz, Y. H. Chen, Y. M. Sun, M. D. Hou, X. H. Qu, L. Zhang and Y. F. Chen, *Nanotechnology*, 2010, **21**, 365605.
18 N. Cabrera and N. F. Mott, *Rep. Prog. Phys.*, 1948, **12**, 163.
19 J. C. Yang and G. W. Zhou, *Micron*, 2012, **43**, 1195.

20 S. M. Johnston, A. Mulligan, V. Dhanak and M. Kadodwala, *Surf. Sci.*, 2002, **519**, 57.
21 G. W. Zhou, X. Chen, D. Gallagher and J. C. Yang, *Appl. Phys. Lett.*, 2008, **93**,123104.
22 G. Zhou and J. C. Yang, *J. Mater. Res.*, 2005, **20**, 1684.
23 L. Luo, Y. Kang, Z. Liu, J. C. Yang and G. Zhou, *Phys. Rev. B*, 2011, **83**, 155418.
24 D. Y. Lei, K. Appavoo, F. Ligmajer, Y. Sonnefraud, R. F. Haglund and S. A. Maier, *ACS Photonics*, 2015, **2**, 1306.
25 K. Appavoo, D. Y. Lei, Y. Sonnefraud, B. Wang, S. T. Pantelides, S. A. Maier and R. F. Haglund, *Nano Lett.*, 2012, **12**, 780.
26 D. Y. Lei, K. Appavoo, Y. Sonnefraud, R. F. Haglund and S. A. Maier, *Opt. Lett.*, 2010, **35**, 3988.
27 D. Y. Lei, A. I. Fernández-Domínguez, Y. Sonnefraud, K. Appavoo, R. F. Haglund, Jr., J. B. Pendry and S. A. Maier, *ACS Nano*, 2012, **6**, 1380.
28 J. L. Duan, T. W. Cornelius, J. Liu, S. Karim, H. J. Yao, O. Picht, M. Rauber, S. Müller and R. Neumann, *J. Phys. Chem. C*, 2009, **113**, 13583.
29 C. Wang, M. Zhang, H. Wang, S. Zou and M. Su, *J. Phys. Chem. Lett.*, 2010, **1**, 79.
30 L. S. Jung, C. T. Campbell, T. M. Chinowsky, M. N. Mar and S. S. Yee, *Langmuir*, 1998, **14**, 5636.
31 J. C. Yang, B. Kolasa and J. M. Gibson, *Appl. Phys. Lett.*, 1998, 73, 2841.
32 M. E. Toimil Molares, *Beilstein J. Nanotechnol.*, 2012, **3**, 860.
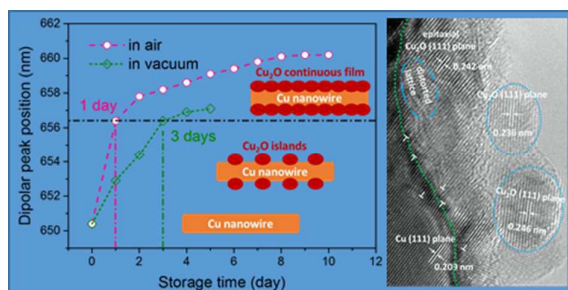
Surface plasmonic spectroscopy reveals the oxidation dynamics of copper nanowires embedded in polycarbonate ion-track templates. A method is proposed to prevent natural oxidation of metal nanostructures in general.